JOURNAL OF MATERIALS RESEARCH AND TECHNOLOGY 2023;24:2812–2827

Available online at www.sciencedirect.com

jmr&t
Journal of Materials Research and Technology

journal homepage: www.elsevier.com/locate/jmrt

Probabilistic fatigue estimation framework for aeroengine bladed discs with multiple fuzziness modeling

Yao-Wei Wang [a], *Lu-Kai Song* [b,c,*], *Xue-Qin Li* [a], *Guang-Chen Bai* [a]

[a] *School of Energy and Power Engineering, Beihang University, Beijing, 100191, China*
[b] *Department of Mechanical Engineering, The Hong Kong Polytechnic University, Hong Kong, China*
[c] *Research Institute of Aero-Engine, Beihang University, Beijing, 100191, China*

ARTICLE INFO

Article history:
Received 14 December 2022
Accepted 27 March 2023
Available online 30 March 2023

Keywords:
High-cycle fatigue
Fuzzy reliability
Bladed disc
Surrogate model
Support vector regression

ABSTRACT

To reduce the estimation errors of probabilistic fatigue lifetime caused by artificial cognitive factors, a probabilistic fatigue estimation framework with the consideration of multiple fuzziness (i.e., stress and strength) is proposed. In the presented framework, a fuzzy variable randomization-based fuzzy least squares support vector regression is proposed in the level of stress fuzziness, a fuzzy strength model with average stress calibration is established in the level of strength fuzziness, and the corresponding sampling-based probabilistic fatigue estimation framework is given. By regarding a typical compressor bladed disc with titanium-based superalloy as a case, the proposed framework is validated. Methods comparison shows that the proposed approach holds the highest estimation accuracy compared with the methods that do not consider fuzziness of stress or strength. The current efforts develop a novel approach to evaluate the probabilistic fatigue lifetime by fuzzy set theory, which also sheds a light on the reliability-based fatigue design of complex structures.

1. Introduction

High cycle fatigue failure is the most common failure mode of aeroengine compressor bladed discs, and it is one of the most difficult challenges that has plagued numerous generations of aeroengine development [1–3]. According to the aero statistics, high cycle fatigue failure of bladed discs accounts for about 25% of all accidents [4–6]. The development of aeroengines has focused heavily on how to reduce the probability of high cycle fatigue failure of bladed discs, lower the cost of unscheduled aeroengine maintenance, and improve the flight safety. Hereto, researchers have studied methods to improve the fatigue performance from multiple perspectives such as materials and structures [7–10]. However, it is impractical to solely rely on experimental means to address the problem of high cycle fatigue failure in the development process, and the probabislitc estimation techniques for bladed discs are needed to provide guidance. This is because the high cycle fatigue test of the actual aeroengine bladed disc consumes a long cycle time and is unaffordably expensive, and the influence of random factors on the fatigue lifetime dispersion is also be easily ignored [11–13]. Probabilistic estimation primarily comprises the response evaluation of stress level and

* Corresponding author.
E-mail address: songlukai29@163.com (L.-K. Song).
https://doi.org/10.1016/j.jmrt.2023.03.196

Abbreviation list

LSSVR	Least squares support vector regression
FLSSVR	Fuzzy Least squares support vector regression
MRE	Mean relative error
RMSE	Root mean square error
SWT	Smith-Watson-Topper
PDF	Probability density function
CDF	Cumulative distribution function
MCS	Monte Carlo simulation
$P_Z(\bullet)$	Fuzzy probability function
$\varphi(\bullet)$	Hilbert space transformation function
$\psi(\bullet)$	Kernel function
$\|\bullet\|$	Norm function
$\Phi(\bullet)$	Standard normal distribution function
y	Logarithmic fatigue lifetime
y^*	Equivalent logarithmic fatigue lifetime
S	Stress level
μ	Logarithmic lifetime mean value
σ	Logarithmic lifetime standard deviation
$\hat{y}_{50}(\bullet)$	Median logarithmic fatigue lifetime function
$t_{1-\frac{\alpha}{2}}(n-1)$	Bilateral α quantile with n degrees of freedom
S_{ar}	Equivalent cyclic symmetric stress amplitude
S_{max}	Maximum stress
S_a	Stress amplitude
S_m	Average stress
P_s	Survival probability

fatigue modeling of strength level, namely stress response evaluation and fatigue strength assessment. In this regard, relevant scholars have conducted extensive studies, yielding more productive outcomes [14–18].

At the level of stress response evaluation, given the long computing time of structural responses, the construction of surrogate models representing the mapping connection between input variables and output response is the common method for doing efficient evaluation [19–23]. Currently, in response to the conflict between accuracy and efficiency brought on by the complicated and high-nonlinearity stress response assessment, several surrogate model approaches with ensured correctness have been presented one after another. For example, Niu et al. combined reliability theories and sampling techniques to establish a fatigue reliability framework for multivariate uncertainty problems including geometric dimensions [24]; Zhu et al. developed a computational-experimental framework for fatigue reliability assessment and presented a comprehensive uncertainty quantification procedure to quantify multiple types of uncertainty [25,26]; Gao et al. combined Kriging models with substructure techniques in structural dynamics, to propose an efficient probabilistic analysis method for bladed disc composite lifetime [27]; For the dynamic fatigue reliability of integrally bladed discs, Zhang et al. built a generalized regression extremum neural network and examined the fatigue reliability under the influence of thermo-solid coupling loads [28]; Song et al. proposed a distributed collaborative wavelet neural network based on the error control technique for the probabilistic fatigue lifetime assessment of turbomachinery [29]; By combining surrogate model into cooperative design, Meng et al. developed a framework for reliability optimization of turbine blades, offering a creative way to lessen the high computational tasks associated with interdisciplinary optimization [30].

At the level of fatigue strength assessment, researchers have proposed a set of fatigue models and calibrated models for complicated load states of material standards. For example, Walls et al. suggested a high cycle fatigue crack expansion model for bladed discs based on fatigue fracture theory, measuring the relationship between the stress intensity factor and the crack length [31]; Hou et al. established a power-law lifetime model based on crystallography to study the fatigue lifespan of a nickel-based single crystal bladed disc [32]; Zhang et al. developed a high cycle fatigue model for predicting the bladed disc fatigue lifetime induced by aerodynamic loads [33]; Han et al. projected the safe service lifetime of bladed discs with residual lifetime using the calibration technique of probabilistic characteristic parameters [34]; Zhu et al. yield an ultrahigh cycle probabilistic fatigue lifetime prediction model under size effect based on calibrated weakest-link theory by taking the defect factor into account, and the proposed technique is confirmed to be accurate in fatigue lifetime prediction for defective materials [35–38]. In summary, the probabilistic methods and calibrated fatigue models discussed above provide an effective strategy for predicting probabilistic fatigue lifetime for complex structures (i.e., aeroengine bladed discs).

It is believed that the probabilistic properties can accurately describe the uncertainties of variables like material properties, geometric dimensions and suffering loads, and that the information reflected by the test data relied on their fatigue modeling process is sufficient and does not require additional consideration. However, all of these probabilistic methods and models are proposed based on the stochastic framework. In actuality, not all of the aforementioned parameters are always met when predicting the probabilistic high cycle fatigue lifetime of bladed discs [39–42]. For instance, some input variables may not be accurately established or described (i.e., have ambiguity) when modeling the stress response [43–45], such as the rotor speed of a compressor, which is jointly controlled by several systems, and its small fluctuations within the allowable range may exhibit irregular characteristics that cannot be accurately described by a typical probability distribution. Additionally, when modeling strength models, the calibrations to the models may be uncertain due to a lack of information [46–48], i.e., during the calibration of average stress, the small sample test conditions allow for the simultaneous admission of multiple probability patterns of inherent material dispersion at a given confidence level, which results in significant discrepancies between the calculated and true values of calibration parameters [49]. The ambiguities of stress and the non-precision of strengths may be characterized by the fuzziness of probabilistic fatigue model, both of which influence the estimation accuracy. Therefore, it is important to account for the fuzziness of stress and strength, to further improve the estimation accuracy of probabilistic fatigue modeling.

In this case, a probabilistic fatigue estimation framework by considering multiple fuzziness (i.e., stress and strength) is proposed for aeroengine bladed discs. In the presented framework, a fuzzy variable randomization-based fuzzy least squares support vector regression is proposed for stress fuzziness, a fuzzy strength model with average stress calibration is established for strength fuzziness, and the corresponding sampling-based probabilistic fatigue estimation framework is constructed. By regarding a typical compressor bladed disc as a case, the proposed framework is validated. In what follows, Section 2 introduces the basic theory of the proposed estimation framework; the probabilistic fatigue lifetime estimation for a bladed disc is regarded as a validation case in Section 3; some conclusions are summarized in Section 4.

2. Basic theory

In this section, the influence of fuzziness on the probabilistic fatigue lifetime assessment is considered at both stress and strength levels, and a probabilistic estimation framework for high cycle fatigue lifetime is established, including surrogate-based fuzzy stress evaluation, calibration-based fuzzy strength assessment and the specific probabilistic fatigue framework under multiple fuzziness.

2.1. Surrogate-based fuzzy stress evaluation

To address the problem that plentiful input parameters are ambiguous and cannot be accurately described by random probability theory, by combining the fuzzy set theory with the least squares support vector regression (LSSVR) [50–53], a fuzzy LSSVR (FLSSVR) method is proposed, by first realizing the interconversion of fuzzy space and probability space based on the sample prior distribution, and then building the training sample set in probability space for LSSVR fitting. The detailed modeling process of the FLSSVR is summarized as follows.

Assuming that (Ω, F, P) denotes the probability space and $\tilde{A}$ is a fuzzy event in the probability space; for the membership function $\mu_{\tilde{A}}$, the fuzzy probability can be expressed as [54]:

$$P_Z(\tilde{A}) \triangleq \int_{\tilde{A}} dP = \int_{\Omega} \mu_{\tilde{A}}(x)dx \tag{1}$$

When the prior probability density function $f(\cdot)$ of probability event P is integrable, the Eq. (1) can be rewritten as

$$P_Z(\tilde{A}) = \int_{R} \mu_{\tilde{A}}(x|\theta)f(\theta)d\theta \tag{2}$$

According to the normalization of the fuzzy probability (i.e., $P_Z(\Omega) = 1$), the probability density function of the fuzzy event $\tilde{A}$ is obtained as

$$f_{\tilde{A}}(x) = \frac{\mu_{\tilde{A}}(x|\theta)f(\theta)}{\int_{R} \mu_{\tilde{A}}(x|\theta)f(\theta)d\theta} \tag{3}$$

For the fuzzy probability problems with a scarcity of samples, the uniform distribution is normally taken as the cut set distribution, then the above probability density function can be simplified as

$$f_{\tilde{A}}(x) = \frac{\mu_{\tilde{A}}(x)}{\int_{R} \mu_{\tilde{A}}(x)dx} \tag{4}$$

According to the conditions of regularity, normalization and continuity of the probability density function, the distribution function $F_{\tilde{A}}(x)$ of the fuzzy variables is derived as

$$F_{\tilde{A}}(x) = \int_{-\infty}^{x} \frac{\mu_{\tilde{A}}(x)}{\int_{R} \mu_{\tilde{A}}(x)dx} dx \tag{5}$$

Considering the distribution function of any continuous real random variable obeys uniform distribution $U(0,1)$, based on the above probability distribution function, the process of transformation from fuzzy space to probability space can be established by: firstly, replacing the fuzzy input parameter $\tilde{x}$ with $z \sim U(0,1)$, and co sampling between z and random input parameter x to construct equivalent input parameter set (x, z); thenceforth, the input parameter set $\widehat{\mathbf{x}} = (\mathbf{x}, \tilde{\mathbf{x}})$ is acquired by performing $\tilde{\mathbf{x}} = F_{\tilde{A}}^{-1}(\mathbf{z})$; finally, actual sample set $(\widehat{\mathbf{x}}, \mathbf{y})$ is obtained through structural simulation. Based on the built sample set and the LSSVR model, the regression model is mapped from the original space to the high-dimensional space, to realize the mutual transformation of fuzzy space and probability space. Among them, the nonlinear regression function of FLSSVR is expressed as

$$f(\widehat{\mathbf{x}}, \boldsymbol{\omega}) = \boldsymbol{\omega}\varphi(\widehat{\mathbf{x}}) + b \tag{6}$$

where ω denotes the parameter vector. By applying the error 2-norm and the regularization parameter γ to design the loss function, the nonlinear regression problem can be transformed into the optimization problem as

$$\min \|\boldsymbol{\omega}\|^2 + \gamma \sum (y_i - (\boldsymbol{\omega}\varphi(\widehat{\mathbf{x}}) + b))^2 \tag{7}$$

Assuming that the kernel function is $\psi(\mathbf{x}, \mathbf{x}_i) = \langle \varphi(\mathbf{x}), \varphi(\mathbf{x}_i) \rangle$, by employing the Lagrange method, the above optimization problem can be solved by the following linear equation set, i.e.,

$$\begin{bmatrix} 0 & 1 & 1 & \cdots & 1 \\ 1 & \psi(x_1, x_1) + \dfrac{1}{2\gamma} & \psi(x_1, x_2) & \cdots & \psi(x_1, x_n) \\ 1 & \psi(x_2, x_1) & \psi(x_2, x_2) + \dfrac{1}{2\gamma} & \cdots & \psi(x_2, x_n) \\ \vdots & \vdots & \vdots & \ddots & \vdots \\ 1 & \psi(x_n, x_1) & \psi(x_n, x_2) & \cdots & \psi(x_n, x_n) + \dfrac{1}{2\gamma} \end{bmatrix} \times \begin{bmatrix} b \\ \alpha_1 \\ \alpha_2 \\ \vdots \\ \alpha_n \end{bmatrix} = \begin{bmatrix} 0 \\ y_1 \\ y_2 \\ \vdots \\ y_n \end{bmatrix} \tag{8}$$

After acquiring the solutions of the equation set (i.e., a^*, b^*), the FLSSVR model can be obtained as

$$f(\widehat{\mathbf{x}}) = \sum_{i=1}^{n} a_i^* \psi(x, x_i) + b^* \tag{9}$$

Based on the proposed transformation method for fuzzy parameter and its equivalent random parameter, sampling simulation on Eq. (9) can be realized through co-sampling between random parameters and equivalent random parameters of fuzzy parameters.

2.2. *Calibration-based fuzzy strength assessment*

In high cycle fatigue modeling from the material level to the component level, it is frequently necessary to introduce calibration parameters to achieve high-accuracy lifetime prediction. For example, the actual stress loads of considerable structures are asymmetric cyclic loads, which mostly needs to be corrected for average stress. For complex structures like aeroengine bladed discs, the fatigue tests of large quantities of expensive components are not only challenging to be achieved but invariably subject to cognitive factors in few tests, making the model calibration inaccurate. To address this problem, a fuzzy calibrated fatigue dispersion modeling is presented.

2.2.1. *Fatigue dispersion modeling*

Based on the probability quantile consistency principle for logarithmic fatigue lifetime assessment as shown in Fig. 1 [55,56], it is assumed that the logarithmic lifetime of the same batch of specimens at different stress level is situated at the same probability quantile in respective logarithmic lifetime distribution (i.e., lg N ~ $N(\mu, \sigma^2)$), i.e.,

$$P(\lg N_i < y_i) = \Phi\left(\frac{y_i - \mu_i}{\sigma_i}\right) = P\left(\lg N_j < y_j\right) = \Phi\left(\frac{y_j - \mu_j}{\sigma_j}\right) \tag{10}$$

where $y = \lg N$ denotes the logarithmic lifetime of the same specimen; i, j denotes the i-th and j-th stress levels.

A large number of tests show that there is also an approximate linear relationship between the logarithmic lifetime standard deviation σ and the stress level S for the same batch of metal specimens [57,58]. Based on the fitted coefficient k, it can be expressed as

$$\sigma_i - \sigma_j = k\left(S_i - S_j\right) \tag{11}$$

Considering the low dispersion of specimen lifetime at high stress level, the equivalent logarithmic lifetime can be derived by converting the test logarithmic lifetime of each stress level to the logarithmic lifetime at high-stress level S* as

$$y_i^* = \frac{(y_i - \mu_i)\sigma^*}{\sigma_i} + \mu^* = \frac{(y_i - \mu_i)\sigma^*}{\sigma^* + k(S_i - S^*)} + \mu^* \tag{12}$$

where the mean value of logarithmic lifetime is calculated from the median logarithmic lifetime curve $\mu = \widehat{y}_{50}(S)$. Since the parent sample of the equivalent logarithmic lifetime at stress level S* should obey $N(\mu^*, \sigma^{*2})$, the coefficient k can be derived from

$$\frac{1}{n-1} \sum_{i=1}^{n} \left(\frac{(y_i - \mu_i)\sigma^*}{\sigma^* + k(S_i - S^*)}\right)^2 = \sigma^{*2} \tag{13}$$

where n indicates the total number of specimens. For complex and expensive aeroengine bladed discs, it is still difficult to determine the lifetime distribution under a certain stress level by high cycle fatigue test (at least required 15 specimens), namely σ^* in Eq. (13) is difficult to be counted accurately. In this regard, this study proposes a strategy to determine the value of σ^*: considering that the population mean value μ^* of fatigue logarithm lifetime at stress level S^* can be considered as known, the population variance should make the sample mean value pass the hypotheses-test and the calculated standard deviation at each sample should be positive, i.e.,

$$\sigma^{*2} = \frac{1}{n-1} \sum_{i=1}^{n} \left(\frac{(y_i - \mu_i)\sigma^*}{\sigma^* + k(S_i - S^*)}\right)^2$$
$$\text{s.t.} \quad \left| \frac{\sum_{i=1}^{n} \frac{(y_i - \mu_i)\sigma^*}{\sigma^* + k(S_i - S^*)}}{\sqrt{\frac{n}{n-1} \sum_{i=1}^{n} \left(\frac{(y_i - \mu_i)\sigma^*}{\sigma^* + k(S_i - S^*)}\right)^2}} \right| < t_{1-\frac{\alpha}{2}}(n-1) \tag{14}$$
$$\sigma^* + k(S_i - S^*) \geq 0, i = 1, 2, \cdots, n$$

Assuming that the standard deviation solution interval is $(\sigma^*_{\min}, \sigma^*_{\max})$ and $\widehat{\sigma}^*$ denotes the standard deviation of specimen lifetime under stress level S*, then the σ^* can be obtained as

$$\begin{cases} \sigma^* = \sigma^*_{\min}, \widehat{\sigma}^* < \sigma^*_{\min} \\ \sigma^* = \sigma^*_{\max}, \widehat{\sigma}^* > \sigma^*_{\min} \\ \sigma^* = \widehat{\sigma}^*, \text{otherwise} \end{cases} \tag{15}$$

2.2.2. *Calibrated fatigue model*

Taking into account the limited sample size certainly raises the probability of evaluation bias, which leads to large dispersion assessment mistakes. In this context, considering that the errors in the calibrated model are mathematically reflected in the cognitive uncertainty of model parameters, we employ the fuzzy calibration parameters, instead of deterministic calibration parameters, to establish a fuzzy calibrated model. Herein, the Walker calibrated model [59,60] is adopted as the basis for deriving the fuzzy calibrated modeling, i.e.,

$$S_{ar} = S_{\max}^{1-\gamma} S_a^{\gamma} \tag{16}$$

where $S_{\max}$ denotes the maximum stress at weak site; S_a the stress amplitude; S_{ar} the equivalent cyclic symmetric stress amplitude, i.e., the stress level S under stress ratio $R = -1$; γ the calibration factor of average stress, belongs to (0.4, 0.8).

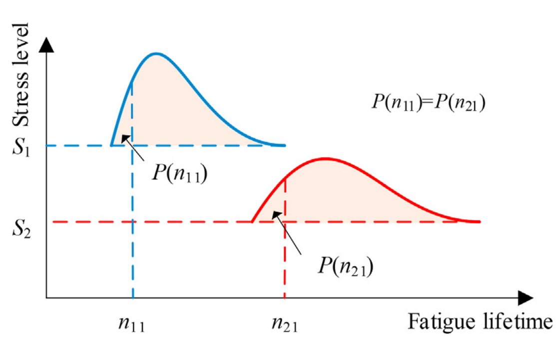

Fig. 1 – Probability quantile consistency principle.

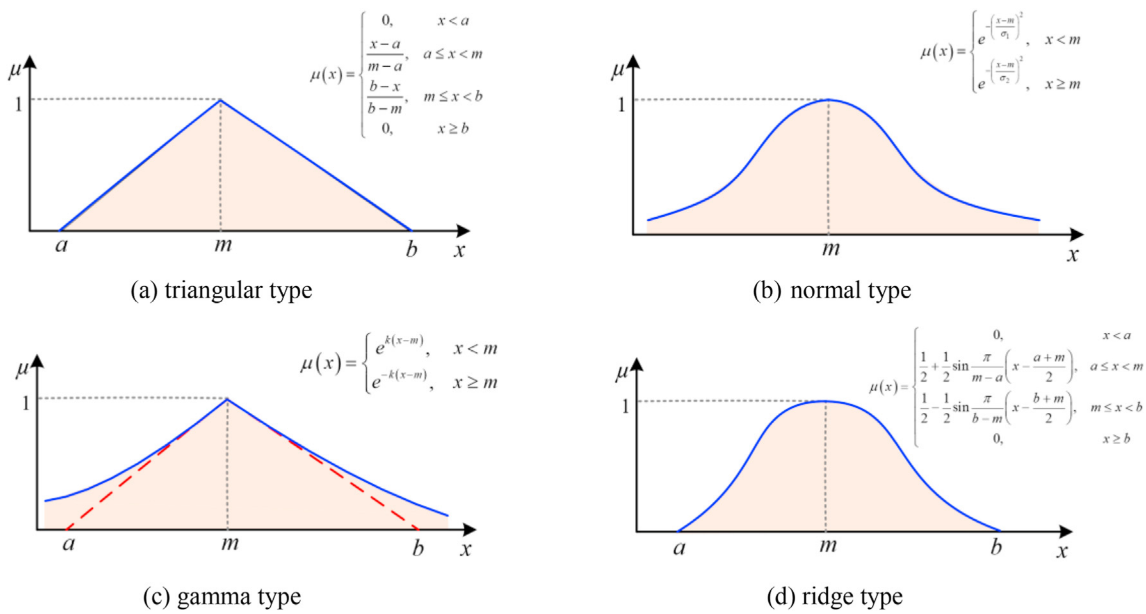

Fig. 2 – Probabilistic characteristics of membership functions.

Based on the fatigue dispersion modeling in section 2.2.1, the mean value and standard deviation of logarithmic lifetime is

$$\begin{cases} \mu(S_{ar};\gamma) = \widehat{y}_{50}\left(S_{\max}^{1-\gamma}S_a^{\gamma}\right) \\ \sigma(S_{ar};\gamma) = k\left(S^* - S_{\max}^{1-\gamma}S_a^{\gamma}\right) + \sigma^* \end{cases} \tag{17}$$

Moreover, the equivalent logarithmic lifetime of the transformation of the test sample values to the stress level S^* can be expressed as

$$y_i^* = g(\gamma) = \frac{\left(y_i - \widehat{y}_{50}\left(S_{\max,i}^{1-\gamma}S_{a,i}^{\gamma}\right)\right)\sigma^*}{k\left(S^* - S_{\max,i}^{1-\gamma}S_{a,i}^{\gamma}\right) + \sigma^*} + \mu^* \tag{18}$$

when γ is a fuzzy variable, the equivalent logarithmic lifetime can be considered as a random variable with a conditional probability density, i.e.,

$$f_i(y_i^*|\tilde{\gamma}) = \frac{1}{\sqrt{2\pi}\sigma^*}e^{-\frac{(g(\gamma)-\mu^*)^2}{2\sigma^{*2}}} \tag{19}$$

Considering that the empirical or calibration parameters in the calibrated model are usually regarded as the fixed values, the commonly applied *L-R* membership functions [61,62] (including triangular type, normal type, gamma type, and ridge type) are used, whose median point m and shape parameters θ are shown in Fig. 2.

Given that the classical set is a special case of the fuzzy set, the Walker calibration parameters can thus be viewed as derived from the fuzzy sample set with constant eigenvalues of 1. Therefore, when the median value of the membership function m is difficult to obtain by fuzzy statistics, the optimal parameter in the classical set can be used as the median point in the fuzzy set with the membership degree of 1, i.e., the parameter value can be estimated by minimizing the sum of squared residuals (SSE) of the median S–N curve

$$m = \underset{\gamma}{\text{argmin}} \quad \sum\left(N_i - \widehat{N}_{50,i}\right)^2 \tag{20}$$

$$\text{s.t.} \quad 0.4 < \gamma < 0.8$$

According to the conditional probability density of Eq. (19), the posterior distribution of the fuzzy random calibration parameters can be obtained from the Bayesian equation, i.e.,

$$f(\tilde{\gamma}|\mathbf{y}^*) \propto f(\mathbf{y}^*|\tilde{\gamma})f_{\tilde{\gamma}}(\gamma) \tag{21}$$

where $\mathbf{y}^* = (y_1^*, y_2^*, \ldots, y_n^*)$ indicates the equivalent logarithmic lifetimes, the probability density of fuzzy random variables $f_{\tilde{\gamma}}(\gamma)$ is obtained from Eq. (4). The shape parameters $\boldsymbol{\theta}$ can be derived from the likelihood function:

$$\boldsymbol{\theta}^* = \text{argmax} \quad (\mathbf{y}^*|\tilde{\gamma})f_{\tilde{\gamma}}(\gamma) \tag{22}$$

To solve for the optimal parameter $\boldsymbol{\theta}$*, the equivalent logarithmic lifetime samples are calibrated to the unbiased estimation samples of $N(\mu^*, \sigma^{*2})$. Moreover, from Eq. (18), the probability density of an equivalent logarithmic lifetime is

$$f_i(y_i^*) = f_{\tilde{\gamma}}(g^{-1}(y_i^*)) = \frac{\mu_{\tilde{\gamma}}(g^{-1}(y_i^*))}{\int_{-\infty}^{+\infty}\mu_{\tilde{\gamma}}(g^{-1}(y_i^*))dy_i^*} \tag{23}$$

Therefore, the shape parameter of the fuzzy variables $\tilde{\gamma}$ can be derived by

$$\begin{cases} E(\mathbf{y}^*) = \frac{1}{n}\sum_{i=1}^{n}E(y_i^*) = \frac{1}{n}\sum_{i=1}^{n}\int_{-\infty}^{+\infty}xf_i(x;\theta_1,\theta_2)dx = \mu^* \\ D(\mathbf{y}^*) = \frac{1}{n-1}\sum_{i=1}^{n}\int_{-\infty}^{+\infty}(x - E(\mathbf{y}^*))f_i(x;\theta_1,\theta_2)dx = \sigma^{*2} \end{cases} \tag{24}$$

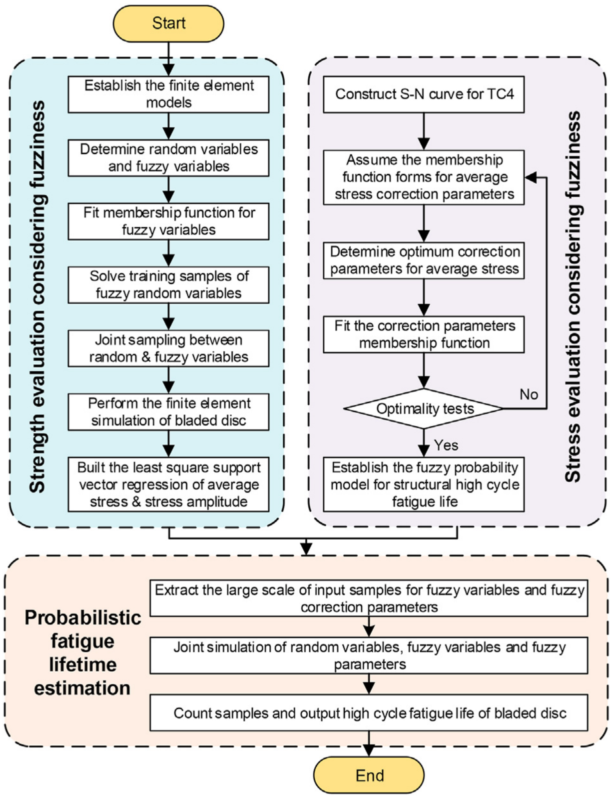

Fig. 3 — Flow chart of the probabilistic fatigue lifetime estimation approach.

To acquire optimal membership function of fuzzy calibration parameters, different forms of membership functions are used and the above fitting process is repeated. The likelihood values of large samples suggest stronger goodness of fit of the calibration parameters, thus producing an average stress fuzzy fatigue model, where the sample likelihood values can be determined by

$$L=\prod_{i=1}^{n}\int_{\tilde{\gamma}}\frac{f_{\tilde{\gamma}}(\gamma)}{\sqrt{2\pi}\sigma(S_{ar,i}|\gamma)}\exp\left(-\frac{(y_i-\mu(S_{ar,i}|\gamma))^2}{2\sigma(S_{ar,i}|\gamma)^2}\right)d\gamma \tag{25}$$

2.3. *Probabilistic fatigue framework under multiple fuzziness*

For any stress level $S=(S_{\max}, S_a)$, the mean value, variance of the log-life distribution can be expressed as

$$\mu=\mu(S_{ar};\tilde{\gamma})=\int_{R}\hat{y}_{50}(S_{ar}|\gamma)f_{\tilde{\gamma}}(\gamma)d\gamma \tag{26a}$$

$$\sigma^2=\int_{R}f_{\tilde{\gamma}}(\gamma)\int_{R}\frac{(x-\mu)^2}{\sqrt{2\pi}\left(k\left(S^*-S_{\max}^{1-\gamma}S_a^{\gamma}\right)+\sigma^*\right)}\exp\left(-\frac{\left(x-\hat{y}_{50}(S_{ar}|\gamma)\right)^2}{2\left(k\left(S^*-S_{\max}^{1-\gamma}S_a^{\gamma}\right)+\sigma^*\right)^2}\right)dxd\gamma \tag{26b}$$

For a given survival probability P_s, the logarithmic lifetime can be calculated by

$$y_P=\mu-k_{p_s,1-\alpha}\sigma \tag{27}$$

where $k_{Ps,1-\alpha}$ represents the one-side tolerance coefficient [63–65]. Since the equivalent probability density function of fuzzy variables $f_{\tilde{\gamma}}(\gamma)$ is usually an atypical distribution function, it is hard to achieve the solution of the variance of Eq. (26). But it is noticed that for each value of fuzzy calibration parameter, the median logarithmic lifetime and its standard deviation can be calculated by the equation below, which provides a way for the statistics of probabilistic fatigue lifetime by sampling.

$$\begin{cases}\mu=\hat{y}_{50}\left(S_{\max}^{1-\gamma_i}S_a^{\gamma_i}\right)\\ \sigma=k\left(S^*-S_{\max}^{1-\gamma_i}S_a^{\gamma_i}\right)+\sigma^*\end{cases} \tag{28}$$

In summary, this paper considers the influence of fuzziness on the probabilistic fatigue lifetime assessment from multiple fuzziness levels: firstly, in terms of stress fuzziness, for the influence of load fuzziness on stress level, a fuzzy variable randomization method with arbitrary membership is established, and a FLSSVR model is proposed; moreover, in terms of strength fuzziness, for the influence of average stress on fatigue strength, a fuzzy average stress calibration coefficient method is proposed, and the corresponding membership function fitting strategy and lifetime calculation method are given; finally, considering stress and strength fuzziness simultaneously, a probabilistic fatigue framework considering stress/strength fuzziness is established, as shown in Fig. 3.

3. Case study: probabilistic fatigue lifetime estimation for bladed disc

In this section, to validate the proposed framework, the probabilistic fatigue lifetime estimation of aeroengine

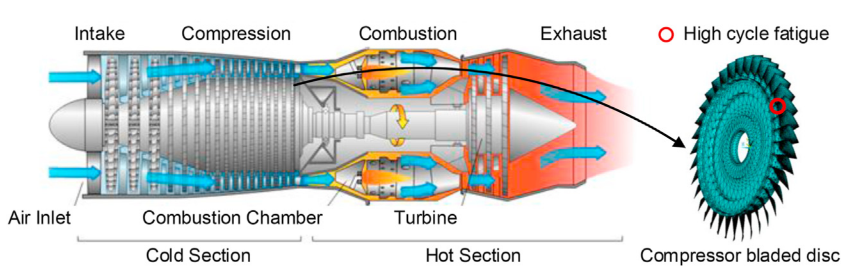

Fig. 4 — Schematic diagram of a typical compressor blade disc.

Table 1 – Distribution characteristics of material parameters.

Random variables	ρ, kg/m^3	E, GPa	G, GPa	α, 10^{-6}, °C	υ
Mean values	4440	109	44	9.1	0.34
Variances	44.4	1.09	0.44	0.091	0.0034

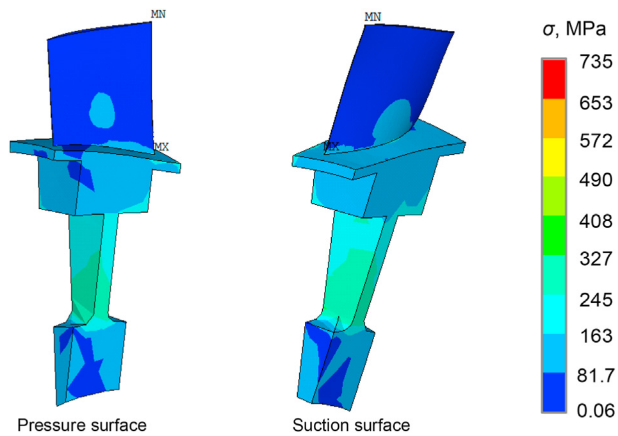

Fig. 5 – Stress distribution on bladed disc under 100% rotational speed.

compressor bladed disc [66] is performed with the consideration of stress/strength fuzziness, the schematic diagram of an aeroengine bladed disc as shown in Fig. 4. It should be noted that all computations are performed on an Inter(R) Core(TM) Desktop Computer (i7-9700K CPU 3.6 GHz and 16 GB RAM).

3.1. *Material preparations*

Given that the randomness of material parameters has a large influence on the fatigue lifetime dispersion of titanium-based superalloy (TC4 material) bladed disc, the material density ρ, elastic modulus E, shear modulus G, expansion coefficient α, and Poisson's ratio υ are considered as the random variables, and their distribution characteristics are shown in Table 1; moreover, according to the compressor speed load spectrum with large fuzzy characteristics, the bladed disc speed is considered as a fuzzy variable with a priori distributed as N(225, 2.25), and its membership function is shown in Eq. (29). By introducing these uncertain variables into the finite element model of the bladed disc, and the deterministic analysis is carried out to derive the stress level of the bladed disc at 100% operating speed (n = 225 r/s). As can be seen in Fig. 5, the maximum stress of the bladed disc occurs at the disc rim site, which reaches 735.17 MPa and is the weakest site where fatigue damage is most likely to occur. Therefore, the probabilistic fatigue lifetime estimation will be carried out subsequently for this weak site.

$$\mu_{\tilde{n}}(x) = \begin{cases} e^{-\frac{(x-225)^2}{2.784^2}}, & x < 225 \\ 1, & x = 225 \\ e^{-\frac{(x-225)^2}{3.344^2}}, & x > 225 \end{cases} \tag{29}$$

3.2. *FLSSVR surrogate modeling*

Based on the numerical characteristics of the uncertain variables, a small number of training samples are extracted. By employing the surrogate modeling strategy proposed in Section 2.1, the surrogate models for average stress $S_m = S_m(\rho, E, G, \alpha, \nu, \tilde{n})$ and stress amplitude $S_a = S_a(\rho, E, G, \alpha, \nu)$ are established. The regression effects and relative errors of the built surrogate models are shown in Figs. 6–7, respectively. To further verify the generalization ability of the built surrogate models, the quantitative indicators like mean relative error (MRE) and root mean square error (RMSE) are introduced in Eq. (30), it is found that the MRE values of the average stress surrogate model and stress amplitude surrogate model are 0.0013 and 0.00021 respectively, and the RMSE values are 1.192 and 0.0311 respectively. Therefore, the built surrogate models are validated to hold high accuracy and can replace the complex nonlinear finite element simulation for efficient and accurate stress level prediction.

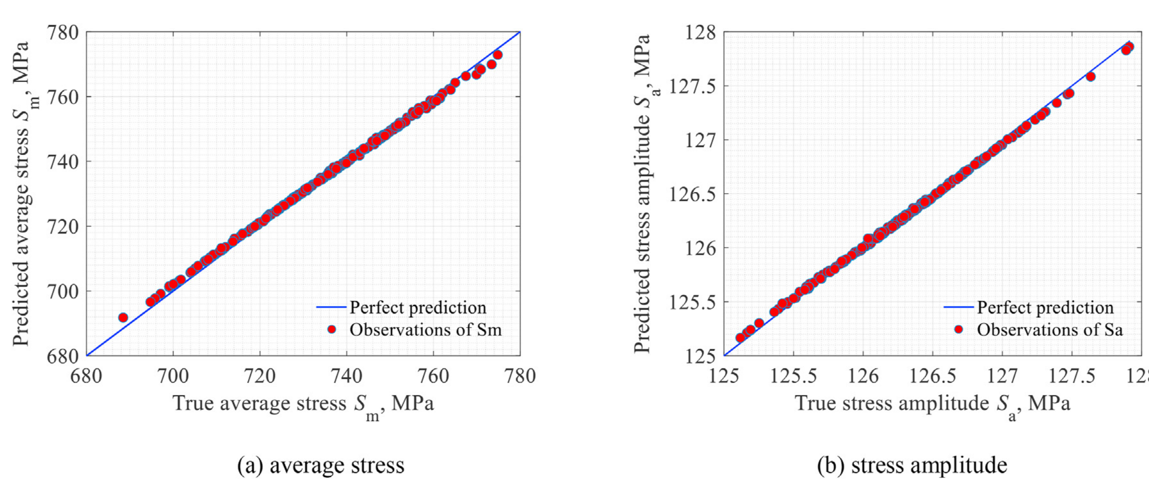

Fig. 6 – Regression effect of the built surrogate model.

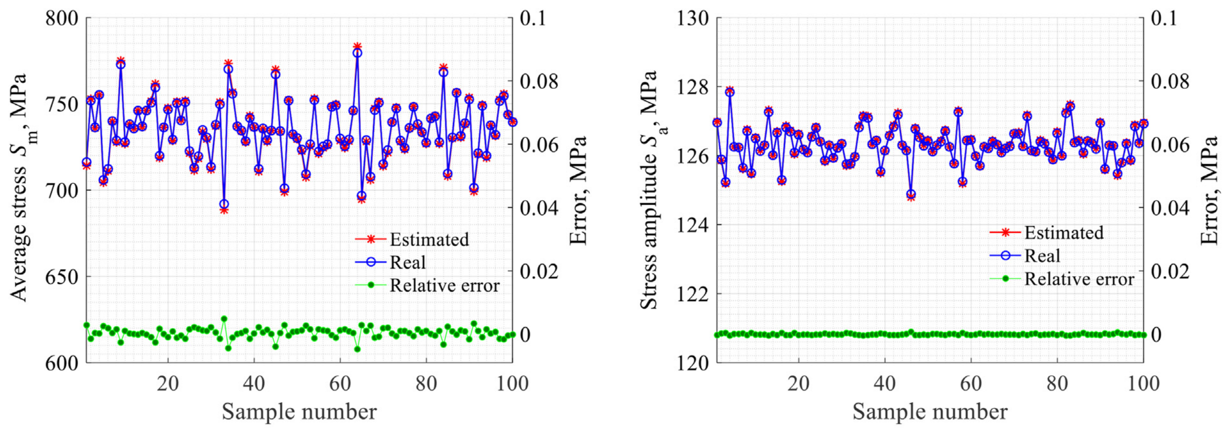

(a) average stress (b) stress amplitude

Fig. 7 – Relative error of the built surrogate model.

Table 2 – Model parameters of the built Walker and SWT models.

Parameter	Walker (R = 0.1)	SWT (R = 0.1)	Walker (R = 0.5)	SWT (R = 0.5)
γ	0.4869	0.5	0.5033	0.5
μ^*	4.1733	4.0460	4.1400	4.1844
σ^*	0.1075	0.1005	0.1685	0.1187

$$\begin{cases} \mathrm{MRE} = \dfrac{1}{n}\displaystyle\sum_{i=1}^{n}\left|\dfrac{x_i - \hat{x}_i}{x_i}\right|, i = 1, 2, \cdots, n \\ \mathrm{RMSE} = \sqrt{\dfrac{1}{n}\displaystyle\sum_{i=1}^{n}(x_i - \hat{x}_i)^2}, i = 1, 2, \cdots, n \end{cases} \tag{30}$$

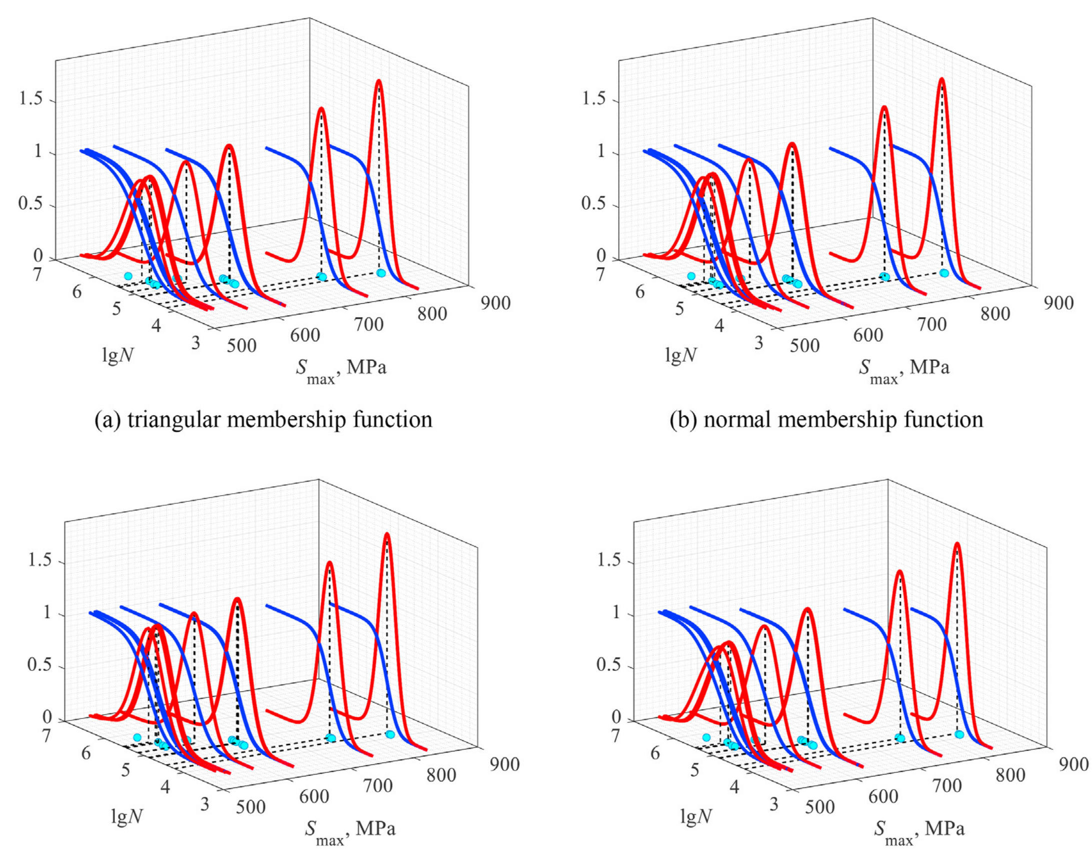

(a) triangular membership function (b) normal membership function

(c) gamma membership function (d) ridge membership function

Fig. 8 – Lifetime distribution under R = 0.1 with different membership functions.

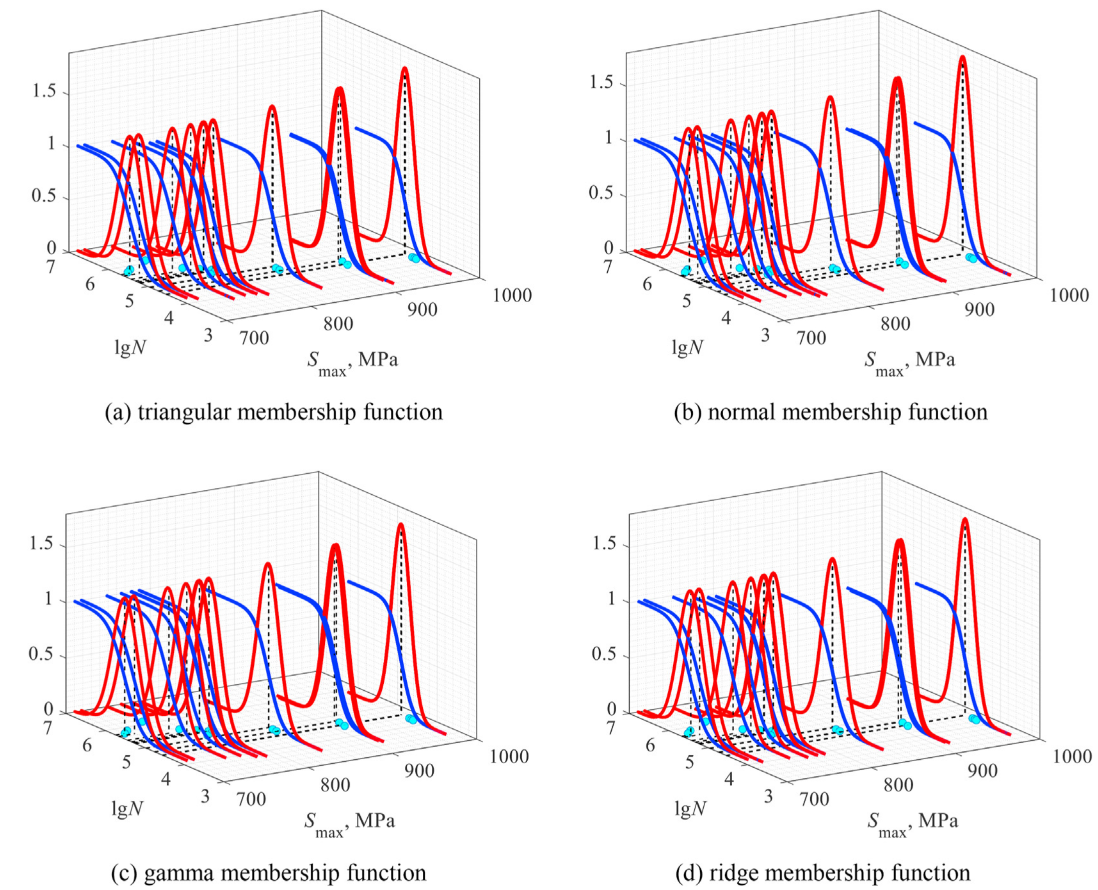

(a) triangular membership function (b) normal membership function

(c) gamma membership function (d) ridge membership function

Fig. 9 – Lifetime distribution under R = 0.5 with different membership functions.

3.3. *Fatigue modeling of TC4 material*

Under the stress ratio $R = -1$ loading conditions, the fatigue lifetime test data of TC4 standard components are shown in Table A in Appendix section [67]. Based on Stromeyer's formulas [68,69], the high cycle fatigue lifetime of TC4 material can be acquired by

$$\lg N = \frac{1}{m}(\lg A + \lg S_0) - \frac{1}{m}\lg(S - S_0) \qquad (31)$$
$$\text{s.t. } S_0 = \text{argmax} \quad r^2$$

where S_0 indicates the model coefficient; r the correlation coefficient. By fitting the test data in Table A with the least

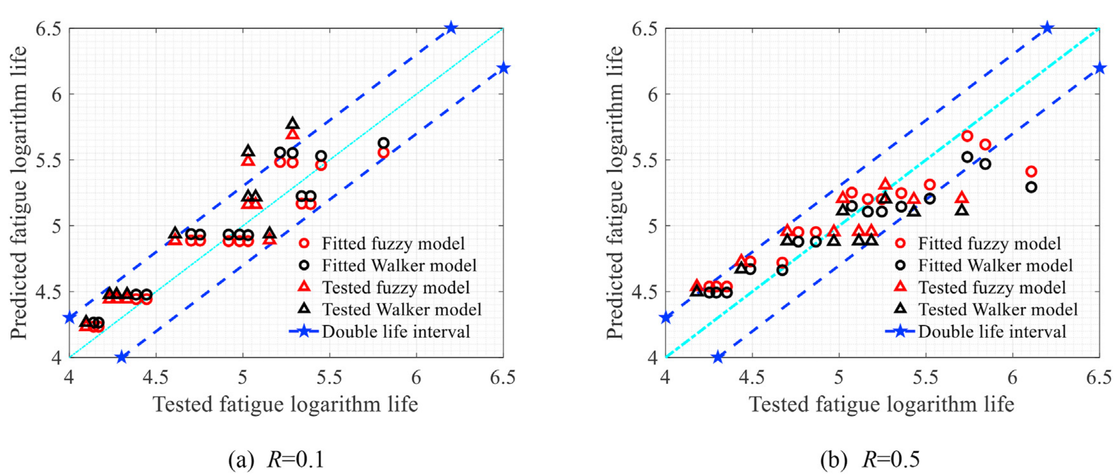

(a) R=0.1 (b) R=0.5

Fig. 10 – Prediction accuracy of the presented fatigue modeling.

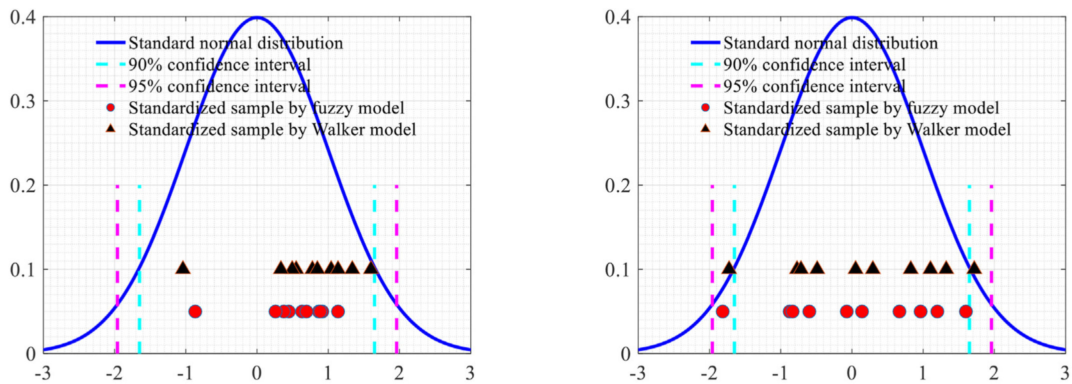

(a) R=0.1 (b) R=0.5

Fig. 11 – Standardized test sample of the probabilistic fatigue modeling.

squares method, the S–N curve of median fatigue lifetime can be established

$$y = \lg N = 9.6060 - 2.2087 \lg(S - 297) \tag{32}$$

According to the presented fatigue dispersion modeling in Section 2.2.1, with a standard deviation slope of $\mu^* = 4.1813$, $\sigma^* = 0.1767$ and $k = -0.0004868$, the logarithmic lifetime distribution at stress level $S^* = 583$ MPa is estimated for the most fatigue lifetime test data among each stress level as is shown in Table A, then the standard deviation of logarithmic lifetime at any stress level can be expressed as

$$\sigma(S) = 0.0004868(583 - S) + 0.1767 \tag{33}$$

By using the fatigue lifetime test data [67] of TC4 material (as shown in Tables B-C in Appendix section) under stress ratio $R = 0.1$ and 0.5 loading conditions: six columns (15 data) on the left side in Tables B-C are used as fitted samples and four columns on the right side are used as test samples, and the fatigue lifetime curve based on the Smith-Watson-Topper (SWT) calibrated model is regarded as the comparison model, as shown in Eq. (34). From the estimation results in Table 2, it is clear that using the average stress calibrated model with given parameters to estimate the lifetime will produce significant errors in calculation results, which, if not addressed, will make it hard to accurately predict the fatigue lifetime of the bladed disc.

$$\begin{aligned} y_{sR0.1} &= \lg N_{R0.1} = 13.0235 - 3.5207 \log\left(\sqrt{S_{\max} S_a} - 228\right) \\ y_{sR0.5} &= \lg N_{R0.5} = 12.6068 - 3.5910 \log\left(\sqrt{S_{\max} S_a} - 283\right) \end{aligned} \tag{34}$$

3.4. *Calibration for fatigue model*

Based on the fatigue test lifetimes with stress ratios of $R = 0.1$ and $R = 0.5$ as shown in Tables B-C, the fatigue model is fuzzified by selecting the membership functions of triangular, normal, Γ and ridge distributions, respectively, and the fatigue lifetime distribution under each stress level at $R = 0.1$ and $R = 0.5$ stress ratios are shown in Figs. 8–9, the corresponding membership functions and maximum likelihood values are shown in Tables D-E in Appendix section, respectively. Herein, the red lines, blue lines, and green dots indicate the probability density function (PDF) curves, cumulative distribution function (CDF) curves, and test data, respectively. From Tables D-E, it is clear that the normal type and the ridge type membership function fits the data best for $R = 0.1$ and $R = 0.5$ respectively, what will be used to create the fuzzy calibrated fatigue model. Note that the test data under two stress ratios are taken to accomplish the fatigue modeling and verify the

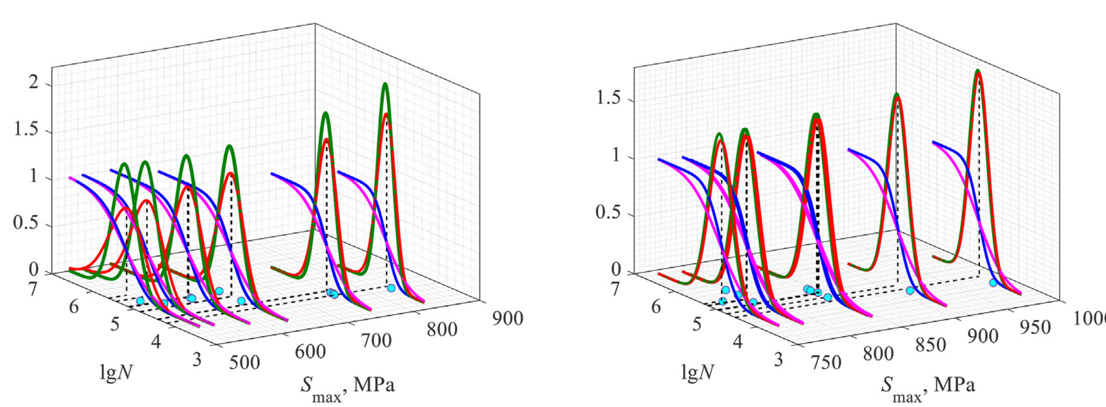

(a) R=0.1 (b) R=0.5

Fig. 12 – Lifetime distribution comparisons of the Walker and the proposed model.

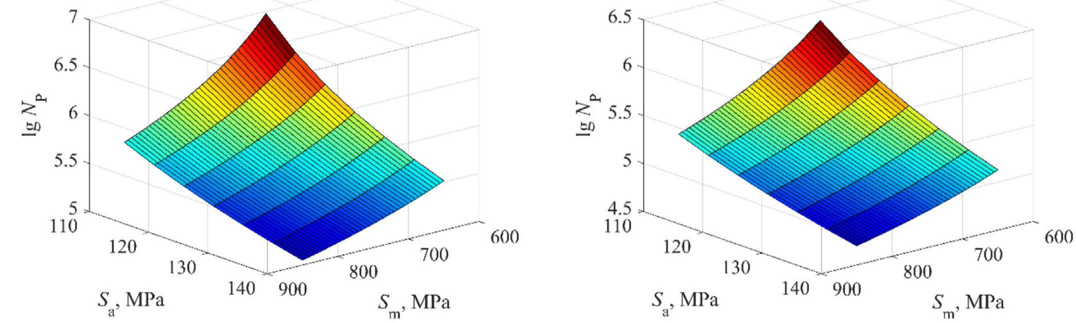

(a) Ps = 50 % (b) Ps = 90 %

(c) Ps = 95 % (d) Ps = 99 %

Fig. 13 – Fatigue strength surface under different survival probability.

superiority of the presented model, which can better illustrate the advantages of the proposed method.

3.5. *Validations for the built fatigue model*

Based on the calibration-based modeling proposed in Section 2.2.2, a fuzzy calibrated fatigue model for TC4 material is developed from fitting data in Tables B-C, its prediction accuracy is shown in Fig. 10. To verify the performance of the constructed fuzzy model in terms of fatigue lifetime distribution estimation, it is compared with the Walker calibrated model, as shown in Figs. 11 and 12. Among them, the green lines and red lines indicate the PDF curves of the Walker calibrated model and the proposed model, respectively; the pink lines and blue lines indicate the CDF curves of the Walker calibrated model and the proposed model, respectively; and the green dots indicate the test data. From the comparison of the lifetime distribution and deviation under the stress ratio $R = 0.1$ and $R = 0.5$, we can observe that the test likelihood values obtained from the fuzzy calibrated

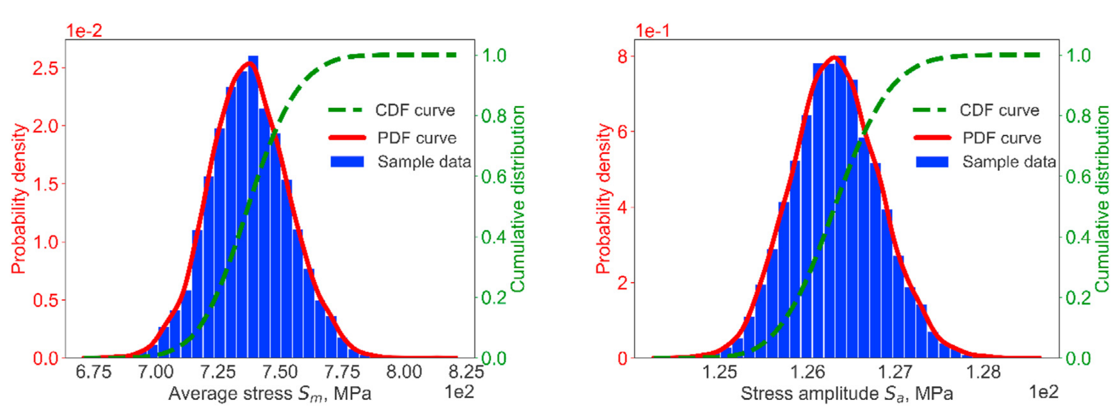

(a) average stress (b) stress amplitude

Fig. 14 – Probabilistic simulation results of stress level.

Table 3 – Estimation results of probabilistic fatigue lifetime.

Numerical traits	Average stress, MPa	Stress amplitude, MPa	Median lifetime, cycles
Mean value	737.47	126.32	4.7822×10^5
Standard deviation	15.828	0.504	4.3266×10^5

model and the Walker calibrated model under the stress ratio $R = 0.1$ are 3.0042 and 1.2681, respectively, and the test likelihood values obtained from the fuzzy calibrated model and the Walker calibrated model under $R = 0.5$ are 0.3561 and 0.3354, respectively, which verifies the fuzzy calibrated model possesses higher evaluation accuracy.

3.6. *Probabilistic fatigue lifetime estimation*

In view of the average stress at weak site of bladed disc is usually much larger than the stress amplitude, the stress ratio $R = 0.5$ test data is chosen to establish the fatigue fuzzy probability model, and the correction coefficient is taken as 1.1 which often belongs 1.1 to 1.3 in engineering practice. When considering both random and fuzzy variables, the probabilistic fatigue model is built as

$$\lg\widehat{N} = 9.6060 - 2.2087\lg\left(1.1\left(S_m(x,\tilde{x}) + S_a(x,\tilde{x})\right)^{1-\tilde{\gamma}} S_a(x,\tilde{x})^{\tilde{\gamma}} - 297\right) \tag{35}$$

Based on lifetime sampling at each stress level, the fatigue strength lifetime curve with given survival probability P_s is shown in Fig. 13. By imported input variables into the built FLSSVR and calibrated fatigue model for 10 000 times, the distributions of average stress, stress amplitude are obtained, as shown in Fig. 14. As shown in Table 3, the average stress and stress amplitude obey normal distributions with mean values of (737.47 MPa, 126.32 MPa) and standard deviations of (15.828 MPa, 0.504 MPa) respectively, and the median lifetime obeys a lognormal distribution with mean value of 4.7822×10^5 cycles and standard deviation of 4.3266×10^5 cycles.

3.7. *Methods comparison*

To verify the effectiveness of the proposed method, the probabilistic fatigue lifetime evaluation results of the proposed method are compared with that of the Monte Carlo simulation (MCS) with regard to stress/strength fuzziness, the MCS only with regard to strength fuzziness and the MCS

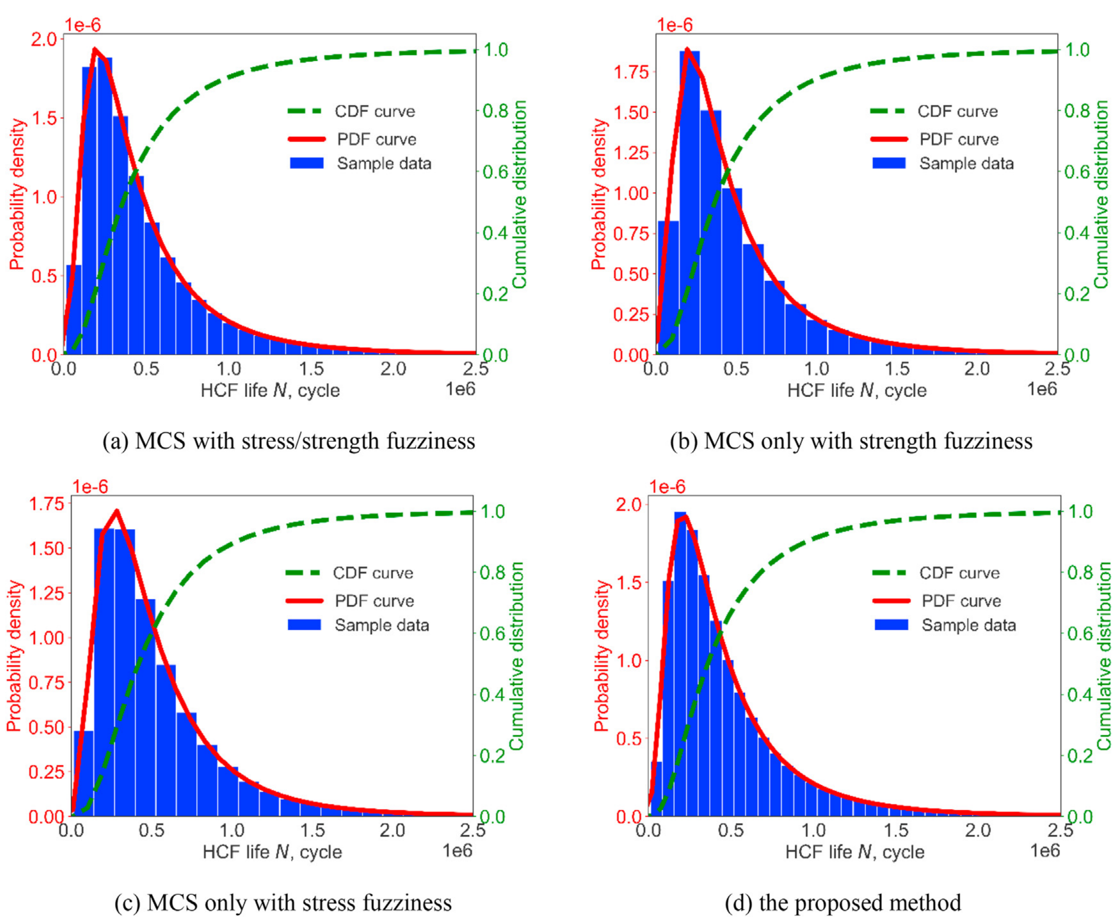

Fig. 15 – Probabilistic fatigue lifetime with regard to fuzziness.

Table 4 – Result comparisons of different simulation methods.

Methods	$P_s = 50\%$		$P_s = 90\%$		$P_s = 95\%$		$P_s = 99\%$	
	Lifetime	Precision	Lifetime	Precision	Lifetime	Precision	Lifetime	Precision
MCS with fuzziness of stress/strength	354 572	–	134 799	–	103 029	–	62 592	–
MCS only with fuzziness of strength	358 281	98.95%	135 861	99.21%	103 749	99.30%	62 925	99.47%
MCS only with fuzziness of stress	414 086	83.22%	168 299	75.15%	130 447	73.39%	80 900	70.75%
The proposed method	354 036	99.85%	134 635	99.88%	102 871	99.85%	62 464	99.79%

without regard to any fuzziness, the corresponding fatigue lifetime distributions obtained using the above methods are shown in Fig. 15. Note that the 5 million group probability fatigue lifetime is calculated by computing the standard deviation of median fatigue lifetime corresponding to each group's average stress and stress amplitude, and then repeated sampling 500 times. Therein, the results of MCS with regard to stress/strength fuzziness are taken as the theoretical truth, the fatigue lifetime and evaluation accuracy under survival probability P_s obtained by each method are shown in Table 4.

As revealed in Table 4, when without regard to stress fuzziness, the calculated fatigue lifetime has errors under each survival probability, and the error of the calculation results gradually increases as the survival probability decreases, which indicates that the stress fuzziness will have a certain influence on the fatigue lifetime evaluation; when without regard to strength fuzziness, the error of fatigue lifetime evaluation under each survival probability increases significantly, which indicates that the accuracy of fatigue lifetime prediction is heavily affected by the fuzziness of strength; The assessment findings of the suggested approach are nearly identical to the MCS with regard to stress/strength fuzziness, its accuracy under each survival probability is more than 99.97%, which proves that the proposed method is an efficient and accurate method for probabilistic fatigue lifetime evaluation of aeroengine bladed discs.

4. Conclusions

To reduce the estimation errors of probabilistic fatigue lifetime caused by artificial cognitive factors, this study considers the fuzzy factors from multiple levels (i.e., stress and strength), proposes a fuzzy least squares support vector regression for fuzzy stress prediction and a fuzzy fatigue strength model with fuzzy calibration parameter, and then combines the two to establish a novel probabilistic fatigue estimation framework. The effectiveness of the proposed approach is verified by taking the probabilistic fatigue estimation of a typical compressor bladed disc as an example, and some conclusions are summarized as follows.

(1) The S–N curve and lifetime distribution of titanium-based superalloy (TC4 material) bladed disc under asymmetric cyclic loading are established, and it is discovered that taking multiple fuzziness into account can significantly improve the accuracy of probabilistic fatigue estimation.
(2) From methods comparison, we discover that the estimation results of the proposed method are similar to those of the Monte Carlo simulation with stress/strength fuzziness, demonstrating the method's benefit of high computing accuracy in probabilistic fatigue estimation.
(3) Considering the deterministic model is a special case of the fuzzy model, the proposed fuzzy modeling and lifetime assessment method can be extended to other fields, like fatigue reliability estimation of complex structures, which are affected by artificial cognitive factors.

Declaration of competing interest

The authors declare that they have no known competing financial interests or personal relationships that could have appeared to influence the work reported in this paper.

Acknowledgements

The current study is co-supported by the National Natural Science Foundation of China (Grant 52105136 and 51975028), the Hong Kong Scholars Program (Grant XJ2022013) and China Postdoctoral Science Foundation (Grant 2021M690290). The authors would like to thank them.

Appendix

Table A – Fatigue test data for TC4 (R = −1) (σ_{max}/MPa , N/cycle)

σ_{max}	N	σ_{max}	N	σ_{max}	N	σ_{max}	N	σ_{max}	N
782.7	3436	582.0	10 486	465.0	45 687	367.9	139 422	337.7	479 085
782.9	3962	582.3	13 615	465.0	50 238	375.5	164 625	358.4	652 278
783.2	5395	584.3	16 076	408.0	75 212	407.2	203 835	366.3	1 099 606
683.5	7521	582.6	18 982	385.9	78 869	407.4	258 447	346.7	2 350 358
683.8	10 486	582.7	21 375	406.8	132 957	348.5	343 623	328.3	2 646 552

Table B – Fatigue test data for TC4 ($R = 0.1$) (σ_{max}/MPa , N/cycle)

σ_{max}	N	σ_{max}	N	σ_{max}	N	σ_{max}	N	σ_{max}	N
834.3	13 755	639.2	56 734	547.9	193 722	834.1	12 515	589.9	107 342
834.3	14 765	639.7	82 784	588.9	218 003	756.6	17 013	547.2	107 342
757.0	24 245	639.9	95 387	589.0	245 326	756.7	18 698	590.0	117 976
757.2	27 935	640.0	107 342	550.2	282 672	756.8	21 544	638.5	142 510
639.1	50 416	547.7	164 204	540.1	646 036	638.8	40 762	527.5	193 722

Table C – Fatigue test data for TC4 ($R = 0.5$) (σ_{max}/MPa , N/cycle)

σ_{max}	N	σ_{max}	N	σ_{max}	N	σ_{max}	N	σ_{max}	N
983.1	17 835	845.3	58 090	778.3	228 546	982.9	15 118	844.4	129 664
983.2	19 602	845.6	73 564	765.7	333 485	913.0	27 283	844.6	152 973
983.4	22 586	777.5	117 976	710.6	547 598	845.1	50 416	766.9	184 785
913.2	30 703	787.0	145 916	718.4	693 467	845.9	93 160	787.7	269 631
915.6	46 967	787.2	176 260	748.8	1 281 422	786.6	104 837	786.7	510 143

Table D – Fuzzy calibration parameter under stress ratio $R = 0.1$

Fuzzy calibration parameter	Membership function	Maximum likelihood value
$\tilde{\gamma}_1$	$\mu(x) = \begin{cases} \frac{x-0.2999}{0.197}, & x \le 0.4869 \\ \frac{0.6548-x}{0.1679}, & x > 0.4869 \end{cases}$	9.7088
$\tilde{\gamma}_2$	$\mu(x) = \begin{cases} \exp\left(-\frac{(x-0.4869)^2}{0.1067^2}\right), & x \le 0.4869 \\ \exp\left(-\frac{(x-0.4869)^2}{0.0955^2}\right), & x > 0.4869 \end{cases}$	11.3714
$\tilde{\gamma}_3$		7.9165
	$\mu(x) = \begin{cases} \exp(21.35(x-0.4869)), & x \le 0.4869 \\ \exp(-21.35(x-0.4869)), & x > 0.4869 \end{cases}$	
$\tilde{\gamma}_4$	$\mu(x) = \begin{cases} 0.5+0.5\sin\left[\frac{\pi}{0.181}(x-0.3964)\right], & 0.3059 < x \le 0.4869 \\ 0.5-0.5\sin\left[\frac{\pi}{0.1622}(x-0.568)\right], & 0.4869 < x \le 0.6491 \end{cases}$	8.3455

Table E – Fuzzy calibration parameter under stress ratio $R = 0.5$

Fuzzy calibration parameter	Membership function	Maximum likelihood value
$\tilde{\gamma}_1$	$\mu(x) = \begin{cases} \frac{x-0.4614}{0.0419}, & 0.4614 \le x < 0.5033 \\ \frac{0.5244-x}{0.0211}, & 0.5033 \le x \le 0.5244 \end{cases}$	0.9490
$\tilde{\gamma}_2$		0.9408
	$\mu(x) = \begin{cases} \exp\left(-\frac{(x-0.5033)^2}{0.0285^2}\right), & x \le 0.5033 \\ \exp\left(-\frac{(x-0.5033)^2}{0.0069^2}\right), & x > 0.5033 \end{cases}$	
$\tilde{\gamma}_3$		0.8505
	$\mu(x) = \begin{cases} \exp(73.67(x-0.5033)), & x \le 0.5033 \\ \exp(-73.67(x-0.5033)), & x > 0.5033 \end{cases}$	
$\tilde{\gamma}_4$	$\mu(x) = \begin{cases} 0.5+0.5\sin\left[\frac{\pi}{0.181}(x-0.3964)\right], & 0.3059 < x \le 0.4869 \\ 0.5-0.5\sin\left[\frac{\pi}{0.1622}(x-0.568)\right], & 0.4869 < x \le 0.6491 \end{cases}$	0.9540

REFERENCES

[1] Kumari S, Satyanarayana DVV, Srinivas M. Failure analysis of gas turbine rotor blades. Eng Fail Anal 2014;45:234–44.

[2] Li XQ, Song LK, Bai GC. Recent advances in reliability analysis of aeroengine rotor system: a review. Int J Struct Integr 2022;13(1):1–29.

[3] Zhang H, Song LK, Bai GC. Active extremum Kriging-based multi-level linkage reliability analysis and its application in aeroengine mechanism systems. Aero Sci Technol 2022;131:107968.

[4] Cowles BA. High cycle fatigue in aircraft gas turbines-an industry perspective. Int J Fract 1989;80(2–3):147–63.

[5] Song LK, Bai GC, Li XQ, Wen J. A unified fatigue reliability-based design optimization framework for aircraft turbine disk. Int J Fatig 2021;152:106422.

[6] Li XQ, Song LK, Bai GC. Physics-informed distributed modeling for CCF reliability evaluation of aeroengine rotor systems. Int J Fatig 2022;167:107342.

[7] Guler O, Varol T, Alver U, Biyik S. The wear and arc erosion behavior of novel copper based functionally graded electrical contact materials fabricated by hot pressing assisted electroless plating. Adv Powder Technol 2021;23(8):2873–90.

[8] Biyik S, Arslan F, Aydin M. Arc-erosion behavior of boric oxide-reinforced silver-based electrical contact materials produced by mechanical alloying. J Electron Mater 2015;44(1):457–66.

[9] Biyik S. Influence of type of process control agent on the synthesis of Ag8ZnO composite powder. Acta Phys Pol, A 2019;135(4):778–81.

[10] Biyik S, Aydin M. Fabrication and arc-erosion behavior of Ag8SnO2 electrical contact materials under inductive loads. Acta Phys Pol, A 2017;131(3):339–42.

[11] Zhang H, Song LK, Bai GC. Moving-zone renewal strategy combining adaptive Kriging and truncated importance sampling for rare event analysis. Struct Multidiscip Optim 2022;65(10):285.

[12] Zhang H, Song LK, Bai GC, Li XQ. Fatigue reliability framework using enhanced active Kriging-based hierarchical collaborative strategy. Int J Struct Integr 2023;14(2):267–92.

[13] Li XQ, Song LK, Bai GC. Deep learning regression-based stratified probabilistic combined cycle fatigue damage evaluation for turbine bladed disks. Int J Fatig 2022;159:106812.

[14] Babich D, Bastun V, Dorodnykh T. Structural-probabilistic modeling of fatigue failure under elastic-plastic deformation. Int J Struct Integr 2019;10(4):484–96.

[15] Zhu SP, Wu YL, Yi XJ, Fu SC, Correia JAFO. Probabilistic fatigue assessment of notched components under size effect using generalized weakest-link model. Int J Fatig 2022;162:107005.

[16] Zhu SP, Foletti S, Beretta S. Probabilistic framework for multiaxial LCF assessment under material variability. Int J Fatig 2017;103:371–85.

[17] Song LK, Bai GC, Li XQ. A novel metamodeling approach for probabilistic LCF estimation of turbine disk. Eng Fail Anal 2021;120:105074.

[18] Li XQ, Song LK, Bai GC. Failure correlation evaluation for complex structural systems with cascaded synchronous regression. Eng Fail Anal 2022;141:106687.

[19] Meng DB, Yang SY, He C, Wang HT, Lv ZY, Guo YP, et al. Multidisciplinary design optimization of engineering systems under uncertainty: a review. Int J Struct Integr 2022;13(4):565–93.

[20] Meng DB, Xie TW, Wu P, Zhu SP, Hu ZG, Li Y. Uncertainty-based design and optimization using first order saddlepoint approximation method for multidisciplinary engineering systems. ASCE-ASME Journal of Risk and Uncertainty in Engineering Systems, Part A: Civil Engineering 2020;6(3):04020028.

[21] Meng DB, Li Y, He C, Guo JB, Lv ZY, Wu P. Multidisciplinary design for structural integrity using a collaborative optimization method based on adaptive surrogate modelling. Mater Des 2021;206:109789.

[22] Li XQ, Song LK, Bai GC. Vectorial surrogate modeling approach for multi-failure correlated probabilistic evaluation of turbine rotor. Eng Comput 2022. https://doi.org/10.1007/s00366-021-01594-2.

[23] Li XQ, Bai GC, Song LK, Wen J. Fatigue reliability estimation framework for turbine rotor using multi-agent collaborative modeling. Structures 2021;29:1967–78.

[24] Niu XP, Wang RZ, Liao D, Zhu SP, Zhang XC, Keshtegar B. Probabilistic modeling of uncertainties in fatigue reliability analysis of turbine bladed disks. Int J Fatig 2021;142:105912.

[25] Zhu SP, Liu Q, Peng W, Zhang XC. Computational-experimental approaches for fatigue reliability assessment of turbine bladed disks. Int J Mech Sci 2018;142–143:502–17.

[26] Zhu SP, Huang HZ, Peng WW, Wang HK, Mahadevan S. Probabilistic Physics of Failure-based framework for fatigue life prediction of aircraft gas turbine discs under uncertainty. Reliab Eng Syst Saf 2016;146:1–12.

[27] Gao HF, Zio E, Wang AE, Bai GC, Fei CW. Probabilistic-based combined high and low cycle fatigue assessment for turbine blades using a substructure-based kriging surrogate model. Aero Sci Technol 2020;104:105957.

[28] Zhang CY, Wei JS, Jing HZ, Fei CW, Tang WZ. Reliability-based low fatigue lifetime analysis of turbine blisk with generalized regression extreme neural network method. Materials 2019;12(9):1545.

[29] Song LK, Bai GC, Fei CW. Probabilistic LCF life assessment for turbine discs with DC strategy-based wavelet neural network regression. Int J Fatig 2019;119:204–19.

[30] Meng DB, Yang SQ, Zhang Y, Zhu SP. Structural reliability analysis and uncertainties-based collaborative design and optimization of turbine blades using surrogate model. Fatig Fract Eng Mater Struct 2019;42(6):1219–27.

[31] Walls DP, deLaneuville RE, Cunningham SE. Damage tolerance based life prediction in gas turbine engine blades under vibratory high cycle fatigue. J Eng Gas Turbines Power 1997;119(1):143–6.

[32] Hou NX, Wen ZX, Yu QM, Yue ZF. Application of a combined high and low cycle fatigue lifetime model on life prediction of SC blade. Int J Fatig 2009;31(4):616–9.

[33] Zhang DY, Hong J, Ma YH, Chen LL. A probability method for prediction on high cycle fatigue of blades caused by aerodynamic loads. Adv Eng Softw 2011;42(12):1059–73.

[34] Han L, Chen C, Guo TY, Lu C, Fei CW, Zhao YJ, et al. Probability-based service safety life prediction approach of raw and treated turbine blades regarding combined cycle fatigue. Aero Sci Technol 2021;110:106513.

[35] He JC, Zhu SP, Luo CQ, Niu XP, Wang QY. Size effect in fatigue modelling of defective materials: application of the calibrated weakest-link theory. Int J Fatig 2022;165:107213.

[36] Ye WL, Zhu SP, Niu XP, He JC, Correia JAFO. Fatigue lifetime prediction of notched components under size effect using critical distance theory. Theor Appl Fract Mech 2022;121:103519.

[37] Liao D, Zhu SP, Keshtegar B, Qian G, Wang QY. Probabilistic framework for fatigue life assessment of notched components under size effects. Int J Mech Sci 2020;181:105685.

[38] Niu X, Zhu SP, He JC, Liao D, Correia JAFO, Berto F, et al. Defect tolerant fatigue assessment of AM materials: size effect and probabilistic prospects. Int J Fatig 2022;160:106884.

[39] Luo C, Keshtegar B, Zhu SP, Taylan O, Niu XP. Hybrid enhanced Monte Carlo simulation coupled with advanced machine learning approach for accurate and efficient structural reliability analysis. Comput Methods Appl Mech Eng 2022;388:114218.
[40] Zhu SP, Keshtegar B, Ben Seghier MEA, Zio E, Taylan O. Hybrid and enhanced PSO: novel first order reliability method-based hybrid intelligent approaches. Comput Methods Appl Mech Eng 2022;393:114730.
[41] Wang BW, Tang WZ, Song LK, Bai GC. Deep neural network-based multiagent synergism method of probabilistic HCF evaluation for aircraft compressor rotor. Int J Fatig 2023;170:107510.
[42] Yang YJ, Wang G, Zhong Q, Zhang H, He J, Chen H. Reliability analysis of gas pipeline with corrosion defect based on finite element method. Int J Struct Integr 2021;12(6):854–63.
[43] Yazgan E, Gurler S, Esemen M, Sevinc B. Fuzzy stress-strength reliability for weighted exponential distribution. Qual Reliab Eng Int 2021;38(1):550–9.
[44] Deng K, Song LK, Bai GC, Li XQ. Improved Kriging-based hierarchical collaborative approach for multi-failure dependent reliability assessment. Int J Fatig 2022;160:106842.
[45] Li XK, Zhu SP, Liao D, Correia JAFO, Berto F, Wang QY. Probabilistic fatigue modelling of metallic materials under notch and size effect using the weakest link theory. Int J Fatig 2022;159:106788.
[46] Kebir T, Correia JAFO, Benguediab M, De Jesus AM. Numerical study of fatigue damage under random loading using Rainflow cycle counting. Int J Struct Integr 2021;12(3):408–18.
[47] Viana CO, Carvalho H, Correia JAFO, Montenegro PA, Heleno RP, Alencar GS, et al. Fatigue assessment based on hot-spot stresses obtained from the global dynamic analysis and local static sub-model. Int J Struct Integr 2021;12(1):31–47.
[48] Liu X, Zhang Y, Xie S, Zhang Q, Guo H. Fatigue failure analysis of express freight sliding side covered wagon based on the rigid-flexibility model. Int J Struct Integr 2021;12(1):98–108.
[49] Terrazas VF, Sedehi O, Papadimitriou C, Katafygiotis LS. A Bayesian framework for calibration of multiaxial fatigue curves. Int J Fatig 2022;163:107105.
[50] Kabir S, Papadopoulos Y. A review of applications of fuzzy sets to safety and reliability engineering. Int J Approx Reason 2018;100:29–55.
[51] Wang BW, Tang WZ, Song LK, Bai GC. PSO-LSSVR: a surrogate modeling approach for probabilistic flutter evaluation of compressor blade. Structures 2020;28:1634–45.
[52] Keshtegar B, Gholampour A, Thai DK, Taylan O, Trung NT. Hybrid regression and machine learning model for predicting ultimate condition of FRP-confined concrete. Compos Struct 2021;262:113644.
[53] Keshtegar B, Yaseen ZM. Reinforcing bar development length modeling using integrative support vector regression model with response surface method: new approach. ISA (Instrum Soc Am) Trans 2022;128:423–34.
[54] Pan CY, Wei WL, Zhang CY, Song LK, Lu C, Liu LJ. Reliability analysis of turbine blades based on fuzzy response surface method. J Intell Fuzzy Syst 2015;29(6):2467–74.
[55] Gu HH, Wang RZ, Zhu SP, Wang XW, Wang DM, Zhang GD, et al. Machine learning assisted probabilistic creep-fatigue damage assessment. Int J Fatig 2022;156:106677.
[56] Barbosa JF, Correia JAFO, Freire RCS, Zhu SP, De Jesus AMP. Probabilistic S-N fields based on statistical distributions applied to metallic and composite materials: state of the art. Adv Mech Eng 2019;11(8). 1687814019870395.
[57] Liu XR, Wang XL, Liu ZH, Chen ZQ, Sun Q. Continuum damage mechanics based probabilistic fatigue lifetime prediction for metallic material. J Mater Res Technol 2022;18:75–84.
[58] Taddesse AT, Zhu SP, Liao D, He JC. Combined notch and size effect modeling of metallic materials for LCF using plasticity reformulated critical distance theory. J Mater Res Technol 2022;18:470–84.
[59] Ozdes H, Tiryakioglu M. Walker parameter for average stress calibration in fatigue testing of Al-7%Si-Mg alloy castings. Materials 2018;10(12):1401.
[60] Lv ZQ, Huang HZ, Wang HK, Gao HY, Zuo FJ. Determining the Walker exponent and developing a modified Smith-Watson-Topper parameter model. J Mech Sci Technol 2016;30(3):1129–37.
[61] Payab M, Khanzadi M. State of the art and a new methodology based on multi-agent fuzzy system for concrete crack detection and type classification. Arch Comput Methods Eng 2021;28(4):2509–42.
[62] Li LY, Lu ZZ, Song SF. Saddlepoint approximation based line sampling method for uncertainty propagation in fuzzy and random reliability analysis. Sci China Technol Sci 2010;53(8):2252–60.
[63] Liao D, Zhu SP, Correia JAFO, De Jesus AMP, Veljkovic M, Berto F. Fatigue reliability of wind turbines: historical perspectives, recent developments and future prospects. Renew Energy 2022;200:724–42.
[64] Wu YL, Zhu SP, Liao D, Correia JAFO, Wang QY. Probabilistic fatigue modeling of notched components under size effect using modified energy field intensity approach. Mech Adv Mater Struct 2021. https://doi.org/10.1080/15376494.2021.1977437. In press.
[65] Zhu SP, Liu Q, Lei Q, Wang QY. Probabilistic fatigue lifetime prediction and reliability assessment of a high pressure turbine disc considering load variations. Int J Damage Mech 2018;27(10):1569–88.
[66] Wang BW, Tang WZ, Song LK, Bai GC. Dynamic meta-modeling method to assess stochastic flutter behavior in turbomachinery. Comput Model Eng Sci 2022;133(1):171–93.
[67] Academic committee of the superalloys, China superalloys handbook[M]. Beijing: China Zhijian Publishing House & Standards Press of China; 2012 [in Chinese)].
[68] Strzelecki P. Accuracy of determined S-N curve for constructional steel by selected models. Fatig Fract Eng Mater Struct 2020;43(3):550–7.
[69] Song CH, Wang HL, Sun ZZ, Wei ZY, Yu H, Chen HB, et al. Effect of multiphase microstructure on fatigue crack propagation behavior in TRIP-assisted steels. Int J Fatig 2020;133:105425.